

A FLEXIBLE SOLVER OF THE HELMHOLTZ EQUATION FOR LAYERED MEDIA

Kurt Otto* and Elisabeth Larsson*

*Uppsala University, Dept. of Information Technology
Box 337, SE-751 05 Uppsala, Sweden
e-mail: Kurt.Otto@it.uu.se, Elisabeth.Larsson@it.uu.se

Key words: Helmholtz equation, preconditioner, object-oriented, underwater acoustics

Abstract. *A flexible solver for the Helmholtz equation is presented. The implementation of the solver is done in an object-oriented style, allowing for easy adaptation to different application problems. The solution methods that are employed are fast compared with standard solution techniques. The viability of the solver is demonstrated for realistic problems in underwater acoustics.*

1 INTRODUCTION

The Helmholtz equation describes wave propagation in applications such as Acoustics¹ and Electromagnetics.² In this paper, we target computational problems in underwater acoustics. Long range acoustic propagation in weakly range-dependent underwater environments with moderate contrasts in density and sound speed at the water/seabed interface is handled appropriately by parabolic equation (PE) methods.¹ However, when the contrasts at the water/seabed interface increase in combination with larger variation in water depth, the accuracy of the PE model becomes a serious concern. This is often the case in the Baltic (especially within the archipelago), where the environment can be strongly range-dependent with local spots of bedrock protruding the sediment. In such environments, the basic one-way propagation assumption of PE models might no longer be valid, since the angles steepen up fast and eventually turn backwards resulting in a backscattered field that no longer is of minor importance. The main advantage of PE approximations is their low computational costs. On the other hand, a Helmholtz solver remains accurate also in regions where PE models may fail, such as regions with large contrasts in the density or the sound speed at the seabed.³

An example of a complex realistic environment in the Stockholm archipelago is found in [4, pp. 20–21]. The water depth varies between 15 and 37 metres and the bedrock protrudes the sediment at the shallowest part. An additional complexity is the presence of gas in the sediment at the deepest part with an expected sound speed as low as 800 m/s. Estimates of the energy balance indicate that the PE model encounters difficulties in the

upslope area, which increase with decreasing frequency. Most probably back-reflections cannot be neglected in this case. To quantify the degree of uncertainty in the PE solution, it would be necessary to invoke a Helmholtz solver.

The topic of this paper is a flexible Helmholtz solver, where flexible indicates both flexibility of the model and of the software, which is implemented in an object-oriented style. Furthermore, as is demonstrated by a comparison with an application specific prototype code, the new flexible solver is both fast and memory lean.

The outline of the paper is as follows. In Section 2, the governing equations are discussed. The radiation boundary conditions that are employed at artificial boundaries are derived in Section 3. Section 4 covers algorithms, software, and performance. Finally, Section 5 shows some application results.

2 GOVERNING EQUATIONS

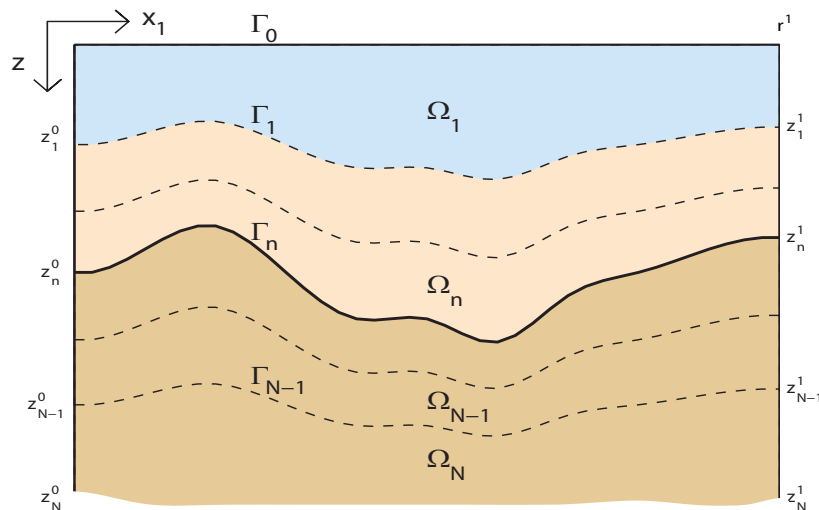


Figure 1: A typical waveguide.

We model time-harmonic sound wave propagation under water. A waveguide consisting of N fluid layers with different densities and sound speeds is considered. The waves are governed by the Helmholtz equation, so within each layer

$$\nabla \cdot \left(\frac{1}{\varrho} \nabla p \right) + \frac{k^2}{\varrho} p = 0, \quad (1)$$

where $p(\mathbf{r})$ is the phasor [2, p. 337] of the acoustic pressure $\text{Re}(p(\mathbf{r}) \exp(-i2\pi ft))$ [1, p. 73] for frequency f , and ϱ is the density of the layered medium. The wavenumber k is given by $k = \frac{2\pi f}{c}(1 + i\delta)$, where the sound speed c and the loss tangent δ may depend on the space

coordinates. In the bottom layer Ω_N , the attenuation (per wavelength) $\beta \equiv 40\pi\delta \log e$ is *required* to be nonzero. The main physical quantities are summarized in the following table.

Symbol	Quantity	Unit
p	acoustic pressure	Pa
f	frequency	Hz
ϱ	density	kg/m ³
c	sound speed	m/s
β	attenuation	dB per wavelength

Table 1: Physical quantities.

The problem is originally three-dimensional but in order to make it computationally tractable, we use either a plane-symmetric or an axisymmetric two-dimensional restriction of the problem. The plane-symmetric or axisymmetric two-dimensional restriction of equation (1) for the layer Ω_d is given by

$$\frac{1}{\eta} \frac{\partial}{\partial x_1} \left(\frac{\eta}{\varrho_d} \frac{\partial p_d}{\partial x_1} \right) + \frac{\partial}{\partial z} \left(\frac{1}{\varrho_d} \frac{\partial p_d}{\partial z} \right) + \frac{k_d^2}{\varrho_d} p_d = 0, \quad (2)$$

where p_d is the acoustic pressure phasor, ϱ_d is the density, and k_d is the wavenumber in the domain Ω_d , $d = 1, \dots, N$. Plane symmetry means that the coordinates (x_1, z) are translated into the Cartesian coordinates (x, y, z) as $x = x_1$, $z = z$, and that the phasor is independent of y . Axial symmetry means that the coordinates are related to cylindrical coordinates (r, φ, z) by $r = x_1 + r^0$, $z = z$, and that the phasor is independent of the azimuthal angle φ . The parameter r^0 (greater than zero for numerical reasons) is the radial distance from the sound source (located on the z -axis) to the near-field boundary ($x_1 = 0$). The scale factor η is given by $\eta = 1$ for plane symmetry and $\eta(x_1) = x_1 + r^0$ for the axisymmetric case.

On the surface boundary Γ_0 , pressure release is imposed. On the interfaces between fluid layers, the pressure and the normal velocity are required to be continuous.

It is assumed that the physical parameters can be grouped into layers with the water layer Ω_1 on top followed by one or several sediment or bedrock layers. The layer interfaces Γ_d are assumed to vary smoothly by range, and the layer thickness must not shrink to zero. Each layer Ω_d is mapped onto a rectangle by an orthogonal transformation⁵ defining boundary conforming coordinates [6, p. 5]. The Helmholtz solver, used in the present work, are stated in those new coordinates. The continuity conditions of pressure and normal velocity can then be treated as for the horizontally stratified case. To damp spurious reflections from the lowermost boundary of the computational domain, an artificial layer Ω_N is added for which the attenuation grows linearly with depth in Ω_N .⁷

3 RADIATION BOUNDARY CONDITIONS

For computational reasons, the range of the domain has to be truncated. For a paraxial approximation⁸ (like PE) that poses no problem, but for a general Helmholtz solver it is a major concern. The truncation is done by introducing a far-field boundary at $x_1 = r^1$ and a near-field boundary at $x_1 = 0$. These artificial boundaries should be transparent to all waves. We emulate this by employing nonlocal Dirichlet-to-Neumann (DtN) maps.⁹

3.1 Normal modes

Boundary conditions based on DtN maps require the boundary in question to be a separable coordinate surface. Our design of radiation boundary conditions follows the principles in.^{10–12} Thus, it is assumed that the bathymetry *beyond* each artificial boundary is horizontally stratified. Under this assumption and the separability requirement that k depends only on the depth z (in the two horizontally stratified regions), the Helmholtz equations (2) can be solved by separation of variables. The ansatz $p(x_1, z) = \chi(x_1)\psi(z)$ leads to separation into the following eigenproblem:

$$-\frac{d}{dz} \left(\frac{1}{\varrho} \frac{d\psi}{dz} \right) - \frac{k^2}{\varrho} \psi = \frac{\lambda}{\varrho} \psi$$

with the boundary conditions taking the form

$$\begin{aligned} \psi(0) &= 0, \\ \psi \text{ and } \frac{1}{\varrho} \frac{d\psi}{dz} &\text{ are continuous at } z = z_d, \quad d = 1, \dots, N-1, \\ \psi(z_N) &= 0, \end{aligned}$$

where N is the number of fluid layers. This Sturm–Liouville problem can be solved numerically by, e.g., Legendre-polynomial FEM^{12,13} or exact finite elements (XFEM)¹⁴ to find an approximant $\tilde{\psi}_m(z)$ to $\psi_m(z)$ and an approximation of λ_m for the m th eigenpair. The propagator $\chi(x_1)$ consists of exponential functions

$$\chi_m(x_1) = A_m \exp(i\sqrt{-\lambda_m}x_1) + B_m \exp(-i\sqrt{-\lambda_m}x_1), \quad m = 1, 2, \dots$$

in the case of plane symmetry, and Hankel functions

$$\chi_m(x_1) = A_m \frac{H_0^{(1)}(\sqrt{-\lambda_m}(x_1 + r^0))}{H_0^{(1)}(\sqrt{-\lambda_m}r^0)} + B_m \frac{H_0^{(2)}(\sqrt{-\lambda_m}(x_1 + r^0))}{H_0^{(2)}(\sqrt{-\lambda_m}r^0)}, \quad m = 1, 2, \dots$$

for axial symmetry. The functions are scaled to yield $\chi_m(0) = A_m + B_m$ for both plane and axial symmetry.

The separated solution $p(x_1, z)$ is a modal sum of $\chi_m(x_1)\psi_m(z)$ over all possible m . For practical reasons the sum must be truncated in an appropriate way. For the DtN

conditions, we devise a truncation based on loss angles [1, p. 134]. Assume that the eigenvalues λ_m are sorted in descending order after $\text{Re}(\sqrt{-\lambda_m})$, and let θ denote the largest allowed loss angle. Modes are included if they satisfy the following attenuation criterion

$$\text{Im}(\sqrt{-\lambda_m}) \leq \min(\tan(\theta)\text{Re}(\sqrt{-\lambda_m}), \alpha),$$

where α is an optional tolerance. The truncation index μ is defined as the highest index for which the attenuation criterion holds. It is different for the near-field (μ_0) and far-field (μ_1) boundaries.

3.2 DtN conditions

The eigenfunctions ψ_m are conjugate with respect to the bilinear form

$$\langle f, g \rangle \equiv \int_0^{z_N} \frac{1}{\varrho} f(z)g(z) dz,$$

which means that $\langle \psi_m, \psi_n \rangle = \delta_{mn}$. This property is used for expressing the coefficients B_m . When r^0 is at least a couple of wavelengths, it is justifiable to associate A_m with waves entering the waveguide at the near-field boundary ($x_1 = 0$). In that case, the coefficients A_m characterize a source term, and we exploit them to *specify* the source as a modal sum. For the extreme near-field, i.e., when r^0 is less than a wavelength, a more sophisticated handling of the source would be necessary.

If we take the bilinear form of the separated solution at $x_1 = 0$ (expressed as a truncated modal sum) and an eigenfunction ψ_m^0 , then because of the conjugacy of the eigenfunctions, we get an expression for the coefficients

$$B_m = \langle \psi_m^0, p(0, \cdot) \rangle - A_m.$$

After differentiating the truncated modal sum with respect to x_1 and eliminating B_m , we obtain the boundary condition

$$-\frac{\partial p}{\partial x_1}(0, z) + \sum_{m=1}^{\mu_0} C_m^0 \langle \psi_m^0, p(0, \cdot) \rangle \psi_m^0(z) = \sum_{m=1}^{\mu_0} A_m^0 \psi_m^0(z), \quad 0 \leq z \leq z_N^0, \quad (3)$$

where

$$C_m^0 = \begin{cases} -i\sqrt{-\lambda_m^0} & \text{for plane symmetry,} \\ -\sqrt{-\lambda_m^0} \frac{H_1^{(2)}}{H_0^{(2)}}(\sqrt{-\lambda_m^0} r^0) & \text{for axial symmetry,} \end{cases}$$

$$A_m^0 = \begin{cases} -2i\sqrt{-\lambda_m^0} A_m & \text{for plane symmetry,} \\ A_m \sqrt{-\lambda_m^0} \left(\frac{H_1^{(1)}}{H_0^{(1)}}(\sqrt{-\lambda_m^0} r^0) - \frac{H_1^{(2)}}{H_0^{(2)}}(\sqrt{-\lambda_m^0} r^0) \right) & \text{for axial symmetry.} \end{cases}$$

The boundary condition at the far-field boundary ($x_1 = r^1$) is derived in a similar way. Due to the anechoic termination of the duct, there are only outgoing waves. Hence, the coefficients $B_m = 0$ and the coefficients A_m are calculated as $A_m = \langle \psi_m^1, p(r^1, \cdot) \rangle$, which results in the condition

$$\frac{\partial p}{\partial x_1}(r^1, z) + \sum_{m=1}^{\mu_1} C_m^1 \langle \psi_m^1, p(r^1, \cdot) \rangle \psi_m^1(z) = 0, \quad 0 \leq z \leq z_N^1, \quad (4)$$

where

$$C_m^1 = \begin{cases} -i\sqrt{-\lambda_m^1} & \text{for plane symmetry,} \\ \sqrt{-\lambda_m^1} \frac{H_1^{(1)}}{H_0^{(1)}} (\sqrt{-\lambda_m^1} (r^1 + r^0)) & \text{for axial symmetry.} \end{cases}$$

4 HELM

Otto and Larsson have *just recently* constructed a flexible HELM (Helmholtz Equation for Layered Media) solver. It can handle two-dimensional restrictions (plane or axial symmetry) of a smoothly varying bathymetry, real or complex wavenumbers, variable material properties, and layered media. The HELM solver is a generalization and comprehensive revision of the prototype FD4HE.⁷

The ingredients of the solution method are fourth-order finite difference¹³ and finite element discretizations, domain decomposition,¹² and preconditioned Krylov subspace methods.¹⁵ In the preconditioner, fast transform subdomain preconditioners¹¹ and the Schur complement algorithm are combined. We use a tensor notation that facilitates the implementation of PDE solvers for discretizations on structured grids. The implementation is made in Fortran 90 employing the framework TENGO (Tensor Notation for Grid Operators). TENGO¹⁶ is written in an object-oriented programming style and contains classes for tensor fields on structured grids, banded linear operators, trigonometric transforms, preconditioners, Krylov subspace methods, etc.

Numerical experiments with FD4HE have been performed on application problems in Acoustics⁷ and Electromagnetics.¹² The memory requirements are low, and the gain in arithmetic complexity compared with standard solution methods is large. The flexibility and computational efficiency of the HELM solver has been demonstrated by comparisons with the prototype (no longer maintained). Figure 2 shows the cpu-time and memory requirements of HELM divided by the corresponding numbers for FD4HE. This means that HELM is actually both faster and less memory demanding than FD4HE for most of the tested problems. However, it should be noted that this is partly due to algorithmic improvements in HELM compared with FD4HE.

5 APPLICATIONS

Figure 3 shows a computation of the transmission loss for the acoustic pressure in an upslope bathymetry with a rigid bottom. The Helmholtz solver employed a computational

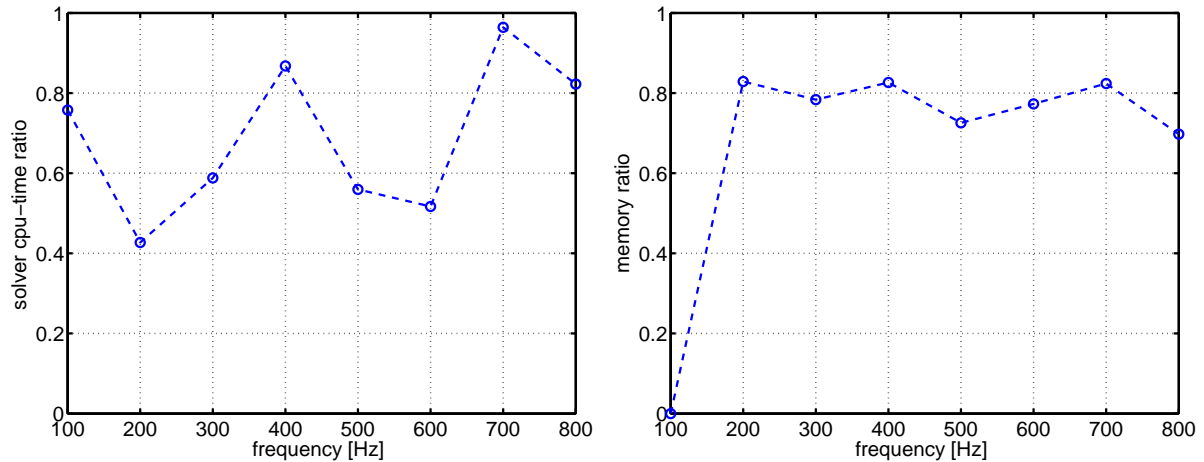


Figure 2: Comparisons with the prototype FD4HE.

grid with 877149 points. A sound speed profile typically arising in the Baltic Sea in the summer was used in the calculation. A monochromatic source triggering the first five propagating modes is located to the left at depth 42 m.

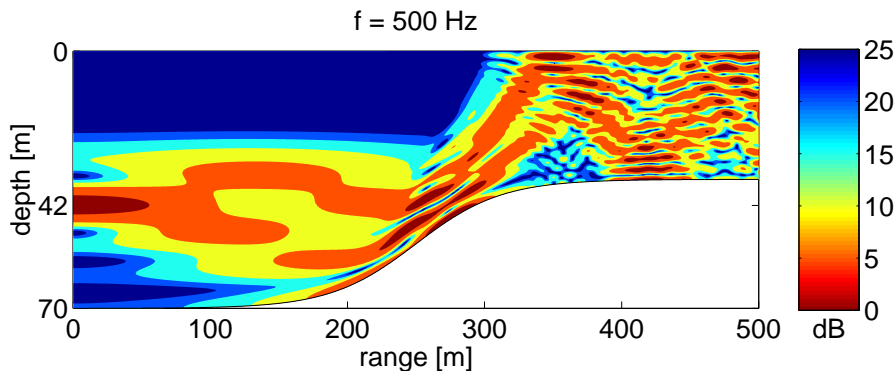


Figure 3: Transmission loss.

The distinct shadow zone in the upper left part of the duct and the sonic channel formed at the source depth are due to the sound speed profile.

REFERENCES

- [1] F. B. Jensen, W. A. Kuperman, M. B. Porter, and H. Schmidt, *Computational Ocean Acoustics*, AIP Press, New York, (1994).
- [2] D. K. Cheng, *Field and Wave Electromagnetics*, Addison-Wesley, Reading, MA, 2nd ed., (1989).

- [3] A. Sundström, Ocean-acoustic test problems with a slowly varying bottom-slope: A missing class of benchmarks, in *Environmental Acoustics*, D. Lee and M. H. Schultz, eds., World Scientific, Singapore, 835–848, (1994).
- [4] L. Abrahamsson and B. L. Andersson, Inversion of seabed parameters in the Stockholm archipelago, Meth. Rep. FOI-R-0300-SE, Division of Systems Technology, Swedish Defence Research Agency, Stockholm, Sweden, (2001).
- [5] L. Abrahamsson, Orthogonal grid generation for two-dimensional ducts, *J. Comput. Appl. Math.*, **34**, 305–314, (1991).
- [6] P. Knupp and S. Steinberg, *Fundamentals of Grid Generation*, CRC Press, Boca Raton, FL, (1993).
- [7] E. Larsson and L. Abrahamsson, Helmholtz and parabolic equation solutions to a benchmark problem in ocean acoustics, *J. Acoust. Soc. Amer.*, **113**, 2446–2454, (2003).
- [8] A. Bamberger, B. Engquist, L. Halpern, and P. Joly, Higher order paraxial wave equation approximations in heterogeneous media, *SIAM J. Appl. Math.*, **48**, 129–154, (1988).
- [9] J. B. Keller and D. Givoli, Exact non-reflecting boundary conditions, *J. Comput. Phys.*, **82**, 172–192, (1989).
- [10] G. J. Fix and S. P. Marin, Variational methods for underwater acoustic problems, *J. Comput. Phys.*, **28**, 253–270, (1978).
- [11] K. Otto and E. Larsson, Iterative solution of the Helmholtz equation by a second-order method, *SIAM J. Matrix Anal. Appl.*, **21**, 209–229, (1999).
- [12] E. Larsson, A domain decomposition method for the Helmholtz equation in a multi-layer domain, *SIAM J. Sci. Comput.*, **20**, 1713–1731, (1999).
- [13] K. Otto, Iterative solution of the Helmholtz equation by a fourth-order method, *Boll. Geof. Teor. Appl.*, **40**:1 suppl., 104–105, (1999).
- [14] I. Karasalo, Exact finite elements for wave propagation in range-independent fluid–solid media, *J. Sound Vibration*, **172**, 671–688, (1994).
- [15] R. W. Freund, G. H. Golub, and N. M. Nachtigal, Iterative solution of linear systems, *Acta Numer.*, **1**, 57–100, (1992).
- [16] K. Åhlander and K. Otto, Software design for finite difference schemes based on index notation, *Future Generation Comput. Syst.*, **22**, 102–109, (2006).